Synthetic Metals
Volume 159, Issues 3-4, February 2009, Pages 325-330

doi:10.1016/j.synthmet.2008.09.011

Balancing the white emission of OLED by a design of fluorescent blue and phosphorescent green/red emitting layer structures

Young Hoon Lee[a], Byung-Kwon Ju[a], Woo Sik Jeon[b], Jang Hyuk Kwon[b], O. Ok Park[c], Jae-Woong Yu[d] and Byung Doo Chin[d],

[a]Display and Nanosystem Laboratory, College of Engineering, Korea University, Seoul 136-713, Republic of Korea

[b]Department of Information Display, College of Sciences, Kyung Hee University, Hoegi-Dong, Dongdaemoon-Gu, Seoul 130-701, Republic of Korea

[c]Department of Chemical and Biomolecular Engineering, Korea Advanced Institute of Science and Technology, 373-1, Guseong-dong, Yuseong-gu, Daejeon 305-701, Republic of Korea

[d]Department of Polymer Science and Engineering, Dankook University, Jukjeon-dong, Suji-gu, Yongin-si Gyeonggi-do, 448-701, Korea

Received 1 April 2008; accepted 16 September 2008. Available online 14 November 2008.

Synthetic Metals 159 (2009) 325–330

Contents lists available at ScienceDirect

Synthetic Metals

journal homepage: www.elsevier.com/locate/synmet

Balancing the white emission of OLED by a design of fluorescent blue and phosphorescent green/red emitting layer structures

Young Hoon Lee[a], Byung-Kwon Ju[a], Woo Sik Jeon[b], Jang Hyuk Kwon[b], O. Ok Park[c], Jae-Woong Yu[d], Byung Doo Chin[d,*]

[a] Display and Nanosystem Laboratory, College of Engineering, Korea University, Seoul 136-713, Republic of Korea
[b] Department of Information Display, College of Sciences, Kyung Hee University, Hoegi-Dong, Dongdaemoon-Gu, Seoul 130-701, Republic of Korea
[c] Department of Chemical and Biomolecular Engineering, Korea Advanced Institute of Science and Technology, 373-1, Guseong-dong, Yuseong-gu, Daejeon 305-701, Republic of Korea
[d] Department of Polymer Science and Engineering, Dankook University, Jukjeon-dong, Suji-gu, Yongin-si Gyeonggi-do, 448-701, Korea

ARTICLE INFO

Article history:
Received 1 April 2008
Accepted 16 September 2008
Available online 14 November 2008

Keywords:
White OLED
Fluorescent and phosphorescent
Broadband emission
Design methods

ABSTRACT

In this paper, we performed the design on the relative thickness of fluorescent–phosphorescent light emitters and evaluated the corresponding change of spectral characteristics of white organic light emitting diode (WOLED). Use of a 3-nm-thick separator composed of undoped phosphorescent host, which provides the confinement of singlet exciton, yields relatively well-defined broadband white emission. The optimized multilayers in WOLED comprises one of the simplest device structures among the reported fluorescent–phosphorescent hybrid WOLEDs, representing the Commission Internationale de l'Eclairage (CIE) 1931 chromaticity ranging from the nearly pure (0.30, 0.35) to warm white (0.35, 0.40) of 9.0–12.5 cd/A (24,000 cd/m^2 at 12 V bias). Although the presented efficiency data is not as high as the reports of others, design principles for a bright and stabilized three-peak-balanced white emission are discussed in detail, which will be beneficial for a step forwards in the development of broadband WOLED.

1. Introduction

White organic light emitting diode (WOLED) has many benefits that can be applicable as a backlight for liquid crystal display, a light source illumination, and the full-color OLED with color filters. With the ability being self-emissive, extremely thin, and light, WOLEDs are particularly suitable for flexible light sources. White light emission at OLED can be obtained from different configuration of devices such as a single-layer blend of polymers comprising red, green, and blue (RGB) light emitting materials [1], multilayered small-molecular organic light emitters of different emissive RGB (red/green/blue) components [2–4], hybrid inorganic/organic composite emitters [5,6], and the excimer with single host–dopant system [7,8]. Depending on the various materials and structural architectures of WOLED, both advantages and disadvantages in terms of the efficiency and stability were extensively discussed [9].

Compared to the relatively low efficiencies of polymeric WOLED, the high efficiency behavior and operational stability of small-molecular WOLEDs are beneficial for a possible commercial application [9–11]. Especially, the high power efficiencies of the WOLED using the electrophosphorescent emitters have been exhibited [12,13] due to the potential harvesting of 100% internal quantum efficiency. However, a shortage of stability of the blue electrophosphorescent emitters limits the stability of white color balance and overall device lifetime of all-phosphorescent WOLEDs [14,15]. Because of the requirement for the host materials with wide bandgap property and the additional electron-blocking layer, it is not easy to design all-phosphorescent WOLEDs with outstanding device stability. An approach to overcome this drawback was the combination of the blue fluorescent emitters and green–red (or orange) phosphorescent emitters [14–16]. This approach includes an initial design of devices preventing the direct energy transfer between the phosphorescent green/red exciton and the non-radiative triplet state of blue emitter. A representative result of Sun et al. shows the performance of 24–37 lm/W at reddish white (0.40, 0.40) [15].

The white emission of a multilayered dye-doped system can be explained with the characteristics of the incomplete energy transfer from the host to the dopant molecules and a uniform distribution of direct carrier trapping at each RGB dopant sites. The singlet energy transfer, that occurs from the excitons formed at the interface of the light-emitting layers and change transport layers, is conspicuous between the host and blue fluorescent dye via the Förster transfer. Since the complete cascade energy transfer results in a

* Corresponding author. Tel.: +82 2 958 5330; fax: +82 2 958 5309.
E-mail address: bdchin@kist.re.kr (B.D. Chin).

0379-6779/$ – see front matter © 2008 Elsevier B.V. All rights reserved.
doi:10.1016/j.synthmet.2008.09.011

single color emission, insertion of the spacer thicker than Förster energy transfer radius (3 nm) provides a confined environment of the fluorescent blue emission at WOLED [14].

Careful design of the relative emission layer thickness in phosphorescent WOLED will maximize the brightness of devices and provide better color balance, while the deviation from pure white (0.33, 0.33) yields the higher efficiency values as seen in many reports [14,15]. Meanwhile, the reported performance near the pure white range (approximately, [0.28, 0.37]–[0.32, 0.30]) are about 10 cd/A [17]. Therefore, for a design of balanced and broadband WOLED aimed for backlight in display, influence of the structural change in the multilayers on the white balance and efficiency should be investigated in more detail. More importantly, simplifying the multilayered RGB WOLED structure is favored while maintaining the balanced broadband spectrum. A uniform distribution of the partial energy transfer in the range of overall RGB-emitting region and trapped charge carriers at each dopant sites are particularly necessary.

In this paper, based on the concept of separated energy transfer for singlet blue and triplet green–red exciton [14–16], we have designed more simplified WOLED structure with broadband spectrum and investigated the factors for balancing spectral characteristics. In order to understand the effect of relative thickness of the emitting layers on the opto-electronic properties of devices such as *I–V* curve, spectral characteristics, and efficiency behavior, results from the screening experimental design methods (factorial) were analyzed, which is unique approach in our report on WOLED. Optimized thickness of the RGB light emitting layers, with the use of single phosphorescent host, was set to yield a balanced white emission and higher brightness behavior at a given condition of device structure.

2. Experimental

The light-emitting layer of WOLED consists of a blue fluorescent dopant (4,4′-bis (9-ethyl-3-carbazovinylene)-1,1′-biphenyl (BCzVBi), green phosphorescent dopant, fac-Tris(2-phenylpyridine)iridium(III)($Ir(ppy)_3$), and Tris[1-phenyliso quinolinato-C_2, N]iridium(III)($Ir(piq)_3$) as a red phosphorescent dopant. As a hole-transport layer (HTL), N,N'-diphenyl-N,N'-bis(1-naphthyl)-(1,1'-biphenyl)-4,4'-diamine (NPB, 40 nm) was vacuum-deposited at 6×10^{-7} Torr onto a UV-O_3 treated indium tin oxide (ITO, 150 nm thickness with a sheet resistance of 30 Ω/sq) substrates. 4,4'-N,N'-dicarbazole-biphenyl (CBP) was selected as a common host material, both for fluorescent and phosphorescent light emitting layers. On top of HTL, blue, green, and red-emitting layers were fabricated with various thickness and doping ratio. In case of devices equipped with a singlet-exciton separator, 3-nm-thick CBP between blue fluorescent and green phosphorescent layer was employed. On top of the red-emitting layer, 4,7-diphenyl-l,10-phenanthroline (Bphen, 25 nm) was deposited as a hole blocking and electron transporting layer, followed by a lithium fluoride (LiF) and an aluminum (Al) cathode. Alternatively, 5-nm-thick hole-blocking layer of aluminum(III) bis(2-methyl-8-quinolinato)4-phenylphenolate (BAlq) was deposited, then a 20-nm-electron transport layer of Tris(8-hydroxyquinoline)-aluminum (Alq_3) and LiF/Al layer were fabricated. The pixel size of the emitting area was 4.0 mm^2. Details of the WOLED device structure are given in Table 1. The luminescence–voltage (*L–V*), current efficiency–voltage characteristics, and spectral characteristics of WOLEDs were measured using a Keithley 236 source measurement unit and CS-1000 spectrometer (Minolta). The energetic barriers of each dopants and host were investigated by the method described elsewhere [18,19]. Fig. 1 shows the chemical structure of used organic materials and device architecture with the relevant energy levels.

3. Results and discussion

Design of the relative thickness structure of white-emitting multilayers was performed; we fixed the thickness and doping ratio of green phosphorescent layer, while the varying parameters were the thickness of the fluorescent blue layer, that of phosphorescent red layer, and the presence of the undoped CBP (singlet-exciton separator). This factorial design has three factors, which have two independent levels ($2 \times 2 \times 2$ groups). The advantages of the factorial design for the parameters in WOLED device are that we can effectively combine a series of independent experiments into one, which cover the simultaneous variation of each parameter, main effect evaluation, and interaction effect (see Table 1, devices 1–8 represent the group of WOLED by statistical experimental design).

The properties of device group with and without the exciton separator (3 nm CBP) are compared in Fig. 2, illustrating the current density/brightness vs. applied voltage bias [(a) and (b)] and efficiency vs. brightness behavior [(c) and (d)]. Excitons that might be formed at the NPB/CBP and Bphen/CBP interfaces [15,16] seem to be efficiently utilized within light-emitting multilayer doped with RGB dopants. Since the role of CBP spacer is to confine the singlet exciton within the blue fluorescent emitting region, general enhancement of brightness devices 5–8 can be explained by the effect of such confinement, which will prevent the energy transfer to lower singlet energy of phosphorescent green dopant and triplet quenching. However, the current (luminous) efficiency was reduced at the devices from 5 to 8, which might be explained by the impeded hole-transport at the devices with CBP separator (compare Fig. 2(c) and (d)). Therefore, the reduction of both current density and brightness at the given voltage bias was observed when each of the thickness of blue- and red-emitting layer was increased. The overall effect of structure design on the brightness and effi-

Table 1
The thickness and dye-doping ratio of the emissive layers of three-layered WOLEDs investigated in this paper. The complete device structure is ITO (10 nm)/NPB (50 nm)/CBP:BCzVBi/*CBP/CBP:$Ir(ppy)_3$/CBP:$Ir(piq)_3$/BPhen (25 nm) [+BAlq (5 nm)/Alq_3 (20 nm)]/LiF/Al.

Device codes	Blue-emitting layer CBP:BCzVBi	Singlet-exciton separator *CBP	Green-emitting layer CBP:$Ir(ppy)_3$	Red-emitting layer CBP:$Ir(piq)_3$
Device 1	5 nm (1.5%)	0	12 nm (7%)	8 nm (7%)
Device 2	5 nm (1.5%)	0	12 nm (7%)	15 nm (7%)
Device 3	10 nm (1.5%)	0	12 nm (7%)	8 nm (7%)
Device 4	10 nm (1.5%)	0	12 nm (7%)	15 nm (7%)
Device 5	5 nm (1.5%)	3 nm	12 nm (7%)	8 nm (7%)
Device 6	5 nm (1.5%)	3 nm	12 nm (7%)	15 nm (7%)
Device 7	10 nm (1.5%)	3 nm	12 nm (7%)	8 nm (7%)
Device 8	10 nm (1.5%)	3 nm	12 nm (7%)	15 nm (7%)
Device 9+	5 nm (1.5%)	3 nm	12 nm (7%)	8 nm (7%)
Device 10+	6 nm (1.5%)	4 nm	15 nm (7%)	10 nm (7%)

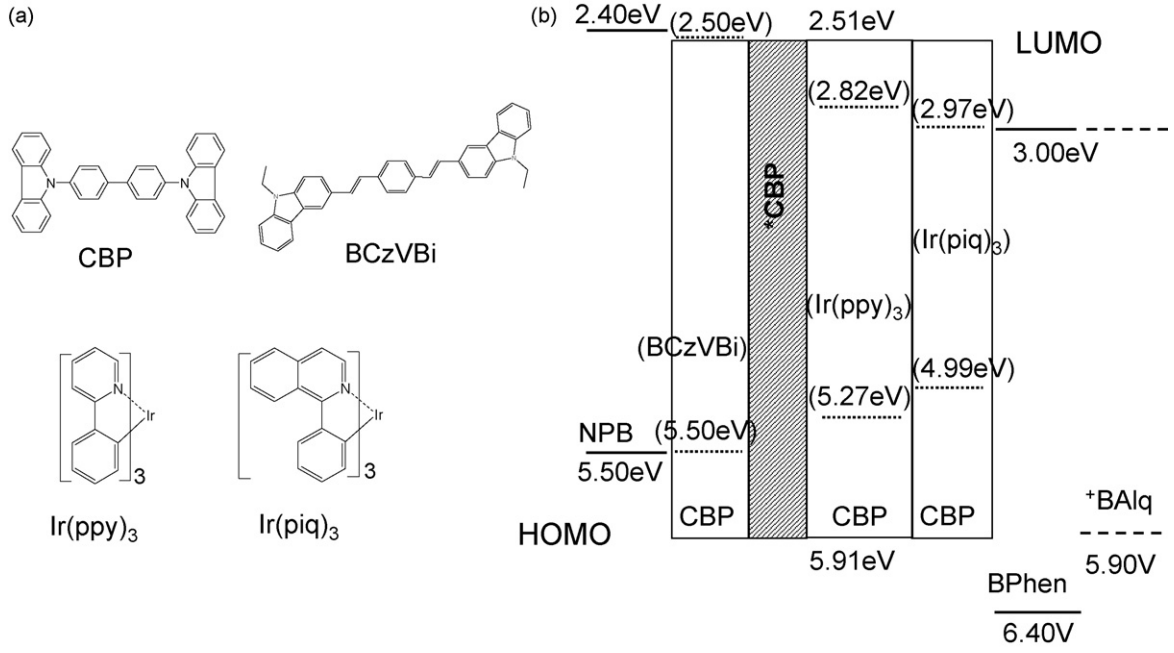

Fig. 1. (a) Materials employed for the light-emitting layer of WOLED; (b) HOMO/LUMO energy level diagram of device with blue/green/red three-peak emitting layers. [*CBP as a singlet-exciton separator. Bphen as hole blocking/electron transport layer of devices 1–8. +BAlq/Alq_3 as hole blocking/electron transport layer of devices 9–10.]

ciency behavior will be discussed later (see Fig. 4). Although not exactly proven by the external quantum efficiency plot, roll-off of the efficiency at high current (brightness) seems to be less significant in case of devices 5–8. Values of the power efficiency, even at the low voltage bias, was not so high (5–6 lm/W) and rapidly reduced as increasing voltage. Relatively high resistance of ITO (30 Ω/sq), large hole injection barrier at ITO/NPB interface (from 4.8 to 5.5 eV), and use of BPhen (for simple structure without hole-

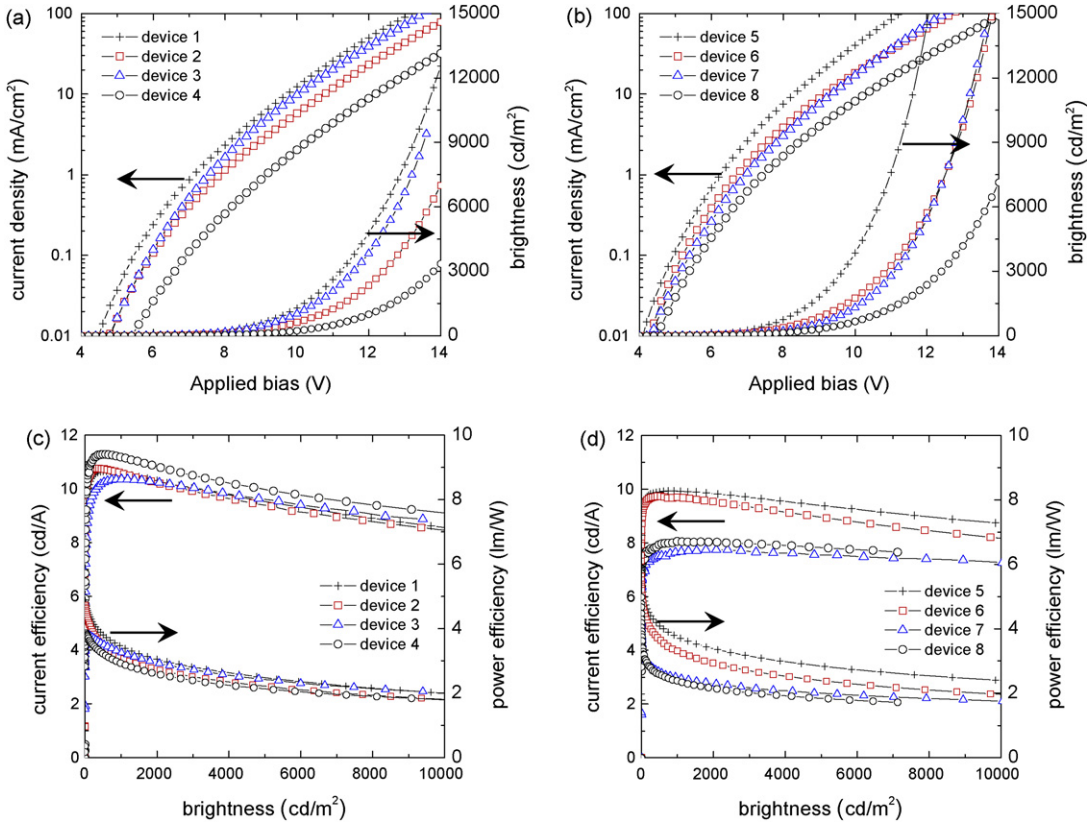

Fig. 2. The device performance of WOLEDs with RGB multilayers; Current density and brightness vs. applied voltage bias behavior for (a) device without CBP singlet-exciton separator; (b) device with CBP separator. Efficiency vs. brightness behavior for (c) device without CBP singlet-exciton separator; (d) device with CBP separator.

blocking layer) might be responsible for such low lm/W efficiency and high operating voltage.

Investigation on the trace of CIE 1931 chromaticity at the variation of applied bias voltage is shown in Fig. 3(a) and (b). The voltage-dependent color index indicates that distribution of exciton recombination region undergoes some change; at low voltage, most of the excitons seem to be formed at the interface between HTL and CBP doped with blue dopant (BCzVBi), while the recombination zone extends for phosphorescent green–red layers at higher voltage bias. Although the color coordinates exhibit the dependence on the bias voltage, devices 1 and 2 with 5 nm blue-emitting layer yield a warm white emission ranging from (0.27, 0.34) to (0.35, 0.45) even without CBP separator. In case of devices with singlet-exciton separator, the intensity of the fluorescent blue emission (confined at CBP:BCzVBi) increases with blue-emitting layer thickness (see the traces of CIE 1931 (x, y) in Fig. 3(b); compared to the devices 5 and 6, one can find the blue-shift of CIE 1931 (x, y) traces in case of devices 7 and 8. However, without the CBP separator, such relationship is not clear due to the disruption of white balance, as seen in Fig. 3(a). This implies that there exists an energy transfer and singlet-exciton diffusion the interface of fluorescent blue/phosphorescent green layer. With CBP separator, pure white emission to the warm white (0.35, 0.40) was achieved, with a reduced voltage-dependence of color purity. Fig. 3(c) and (d) represent the light-emitting spectra of devices 5 and 7, respectively. Relative change of RGB peak intensity was negligible in device 5 (between 5 and 8 V), while the intensity of blue emission is rather suppressed in device 7. The near-pure white emission of 9.65 cd/A, 4.73 lm/W at 100 cd/m^2 (6.4 V) and (0.32, 0.37) was obtained in a multilayered structure of device 5.

The relative position and sequence of the highest occupied molecular orbital (HOMO) and lowest unoccupied molecular orbital (LUMO) energy level of blue/green/red dopant in the CBP host (see Fig. 1(b)), is quite similar with that of blue/green/red fluorescent WOLED [18]. However, the voltage-dependence of color index in the fluorescent–phosphorescent WOLED in our study is diametrically opposed to that of fluorescent WOLED, since the strong bluish emission at high voltage bias is observed in the fluorescent RGB WOLED [18]. At low bias voltage, the singlet exciton formed primarily at the NPB/CBP:BCzVBi interface comprises the bluish white emission, and then as increasing the voltage bias, the unrecombined charge and diffused triplet exciton make further contribution on the green–red phosphorescent emission.

Fig. 4 illustrates the results of the statistical analysis; the dependence of the brightness [(a) and (c)] and efficiency [(b) and (d)] on the layer thicknesses (at the applied bias of 7 V). These trends were universal irrespective of the bias voltage or current densities, whereas the tendency on the shift of color spectrum and CIE 1931 coordinates would be significantly affected by the operation voltage bias. Due to the absence of the point of other experimental data (only boundary points), only a linear expression of the response surface plot was obtained (using Minitab^{TM}). Most noticeably, brightness was decreased considerably with the increase of fluorescent-emitting layer thickness, while the dependence on the red-emitting layer thickness was less pronounced for the group with exciton-blocking layer (c). Similar tendency was observed for

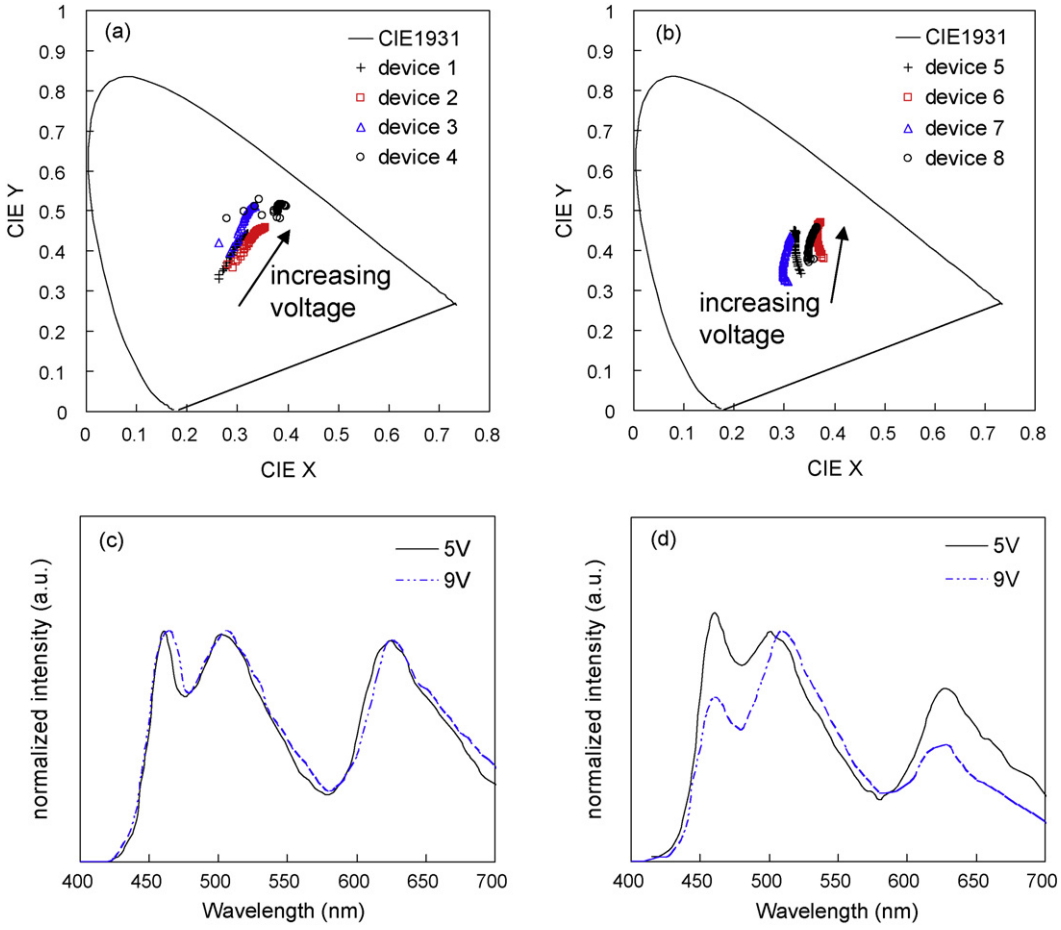

Fig. 3. Trace of the CIE 1931 color coordinates of the WOLEDs with RGB multilayers (a) devices 1–4, without CBP singlet-exciton separator; (b) devices 5–8, with CBP singlet-exciton separator; (c) device 5, electroluminescent spectra at 5 and 9 V; (d) device 7, electroluminescent spectra at 5 and 9 V.

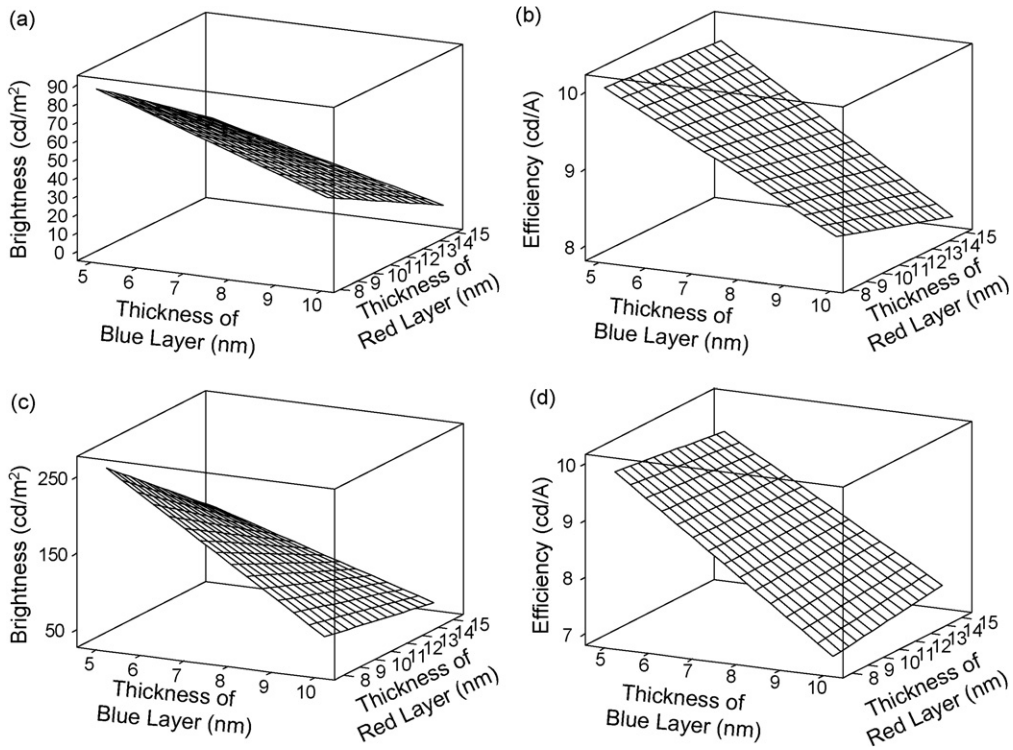

Fig. 4. Surface response plot of the brightness and efficiency of WOLED: dependence on the thickness of fluorescent blue and phosphorescent red emitting layers. (a) analysis of the brightness and (b) efficiency; for a group without exciton separator; (c) brightness and (d) efficiency; for a group with exciton separator.

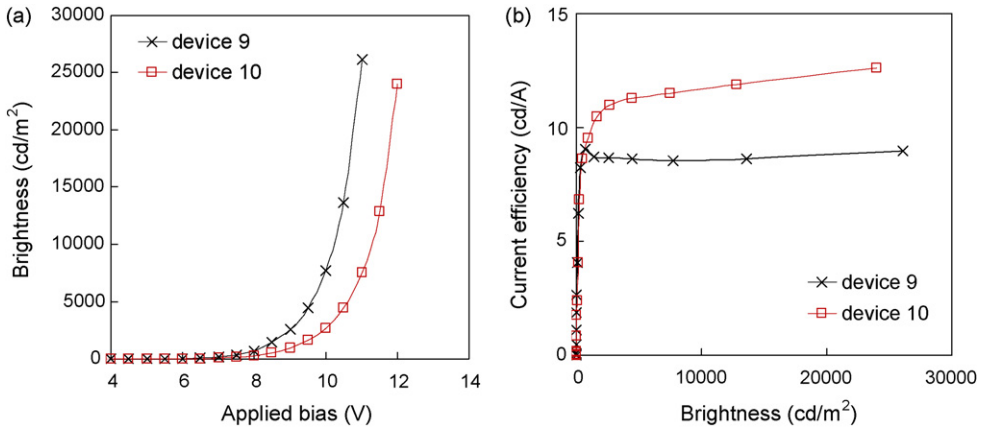

Fig. 5. (a) Brightness vs. applied voltage bias; (b) luminous and power efficiency vs. brightness behavior of WOLED devices 9 and 10.

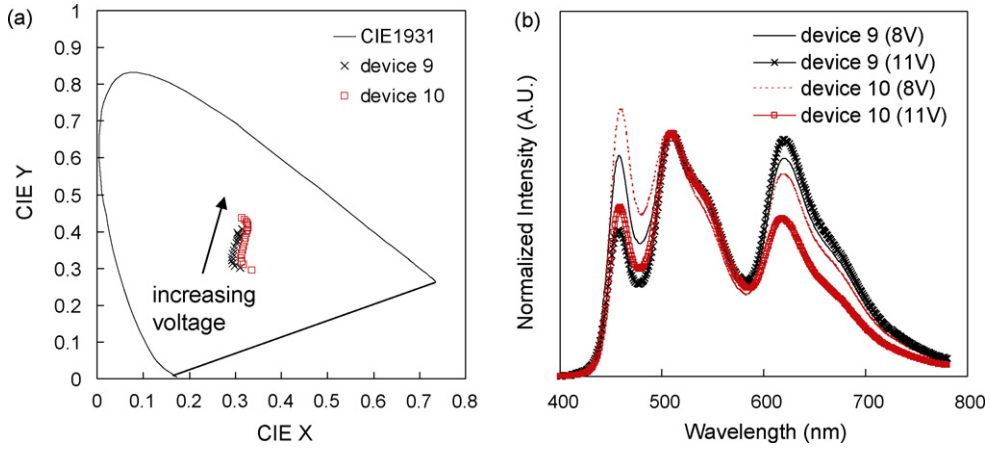

Fig. 6. Variation in the (a) CIE 1931 chromaticity coordinates of three-layered WOLEDs, devices 9 and 10; (b) electroluminescent spectra at 8 and 11 V.

the surface plot of efficiency, indicating that brightness and efficiency were more sensitively responded to the blue-emitting layer thickness than the red-emitting layer thickness. Therefore, it can be concluded that the high energy-emitting layer (here, fluorescent blue) thickness is the most important factor for a design of such hybrid-type WOLEDs.

Generally, higher efficiency is expected upon increasing the overall thicknesses of the light-emitting multilayers. However, the characteristics of broadband white emission depend on the maintenance of optimum balancing in the incomplete energy transfer, carrier trapping, and transport. Fig. 5 shows the effect of overall thickness on the brightness vs. voltage bias and efficiency vs. brightness behavior. Device 9 in Fig. 5 (Here, Bphen is replaced with BAlq/Alq_3) yields the efficiency of 9.03 cd/A at CIE 1931 (0.30, 0.35), which corresponds to the recipe of device 5 (identical emitting layer structure). Slight reduction in efficiency was accompanied, while the lower driving voltage behavior was conspicuous (26,000 cd/m^2 at 11 V, compare with >13 V, as required at device 5). The luminous and power efficiency is further enhanced at device 10 (see Table 1, thicker RGB layers), yielding a value of 12.5 cd/A and 3.3 lm/W at 24,000 cd/m^2. Fig. 6 depicts the CIE 1931 color coordinates and spectral characteristics of devices 9 and 10 at the variation of applied bias voltage. Nearly identical traces of CIE 1931 were produced (reduction of blue-emission intensity at higher voltage), except for the perspective shift of color index, as seen in Fig. 6(a). No bathochromic or hypsochromic shift of electroluminescent spectrum was observed, while the relative intensity of blue fluorescent emission was increased at thicker recipe of device 10 (see Fig. 6(b)). The emission band from the blue fluorescent emitter (BCzVB, 456 nm), green emitter (CBP:Ir$(ppy)_3$, 515 nm), and red emitter (CBP:Ir$(piq)_3$ region, 620 nm) were distinct. From the change of the light-emitting spectra, it can be deduced that distributed recombination region undergo an infinitesimal shift to the short-wavelength region, whereas the characteristic diffusion of triplet exciton into the green–red-emitting layer might not be affected by the thickness variation of blue-emitting layer or separator up to 4-nm thickness.

4. Conclusion

The statistical design method was employed for an optimization of the thickness of stacked fluorescent blue/phosphorescent green/phosphorescent red light emitting layer for WOLEDs with simple structure and reasonable white balance. As reported elsewhere, undoped CBP host was used as a singlet-exciton diffusion barrier and its effectiveness was analyzed in terms of the brightness, efficiency, and color index. While maintaining the characteristic three-peak RGB white emission, relative intensities of blue, green, and red emission were controlled by a variation of the thickness of fluorescent blue and phosphorescent red emitting layer. This design method for each RGB layer and its influence in the device properties and spectral characteristics were discussed in detail. Balanced white emission with three peak ranging from nearly pure white emission (0.30, 0.35) to the warm white (0.35, 0.40) was achieved, yielding 12.5 cd/A at high brightness of 24,000 cd/m^2.

Acknowledgements

The authors acknowledge the Seoul R&BD support program (CR070048). This work was partially supported by GRRC program of Gyunggi province (66944, Development of high efficiency solar cells).

References

[1] J. Kido, H. Shionoya, K. Nagai, Appl. Phys. Lett. 67 (1995) 2281.
[2] B.W. D'Andrade, R.J. Holmes, S.R. Forrest, Adv. Mater. 16 (2004) 624.
[3] X. Jiang, Z. Zhang, W. Zhao, W. Zhu, B. Zhang, S. Xu, J. Phys. D: Appl. Phys. 33 (2000) 473.
[4] B.W. D'Andrade, M.E. Thomson, S.R. Forrest, Adv. Mater. 14 (2002) 147.
[5] J. Feng, F. Li, W. Gao, S. Liu, Y. Liu, Y. Wang, Appl. Phys. Lett. 78 (2001) 3947.
[6] J.H. Park, J.Y. Kim, B.D. Chin, Y.C. Kim, J.K. Kim, O.O. Park, Nanotechnology 15 (2004) 1217.
[7] B.W. D'Andrade, J. Brooks, V. Adamovich, M.E. Thomson, S.R. Forrest, Adv. Mater. 14 (2002) 1032.
[8] E.L. Williams, K. Haavisto, J. Li, G.H. Jabbour, Adv. Mater. 19 (2007) 197.
[9] B.W. D'Andrade, S.R. Forrest, Adv. Mater. 16 (2004) 1585.
[10] P. Spindler, T.K. Hatwar, M.E. Miller, A.D. Arnold, M.J. Murdoch, P.J. Kane, J.E. Ludwicki, S.A. Van Slyke, Society for Information Display (SID) International Symposium Digest, vol. 36, Boston, MA, 2005, p. 36.
[11] N. Ide, T. Komoda, J. Kido, Proc. SPIE 6333 (2006) 63330M.
[12] T. Nakayama, K. Hiyama, K. Furukawa, H. Ohtani, Society for Information Display (SID) International Symposium Digest, vol. 38, Long Beach, CA, 2007, p. 1018.
[13] B.W. D'Andrade, B. Alleyne, M. Hack, R. Hewitt, J.J. Brown, Proc. SPIE 6333 (2006) 63330N.
[14] G. Schwartz, K. Fehse, M. Pfeiffer, K. Walzer, K. Leo, Appl. Phys. Lett. 89 (2006) 083509.
[15] Y. Sun, N.C. Giebink, H. Kanno, B. Ma, M.E. Thomson, S.R. Forrest, Nature 440 (2006) 908.
[16] H. Kanno, N.C. Giebink, Y. Sun, S.R. Forrest, Appl. Phys. Lett. 89 (2006) 023503.
[17] Gangtie Lei, Liduo Wang, Yong Qiu, Appl. Phys. Lett. 88 (2006) 103508.
[18] B.D. Chin, J.K. Kim, O.O. Park, J. Phys. D. Appl. Phys. 40 (2007) 4436.
[19] B.D. Chin, C. Lee, Adv. Mater. 19 (2007) 2061.